Temperature-Dependent Rate Coefficients and Mechanism for the Gas-Phase Reaction of Chlorine Atoms with Acetone

6 AUTHORS, INCLUDING:

Manolis N Romanias
Ecole des Mines de Douai
25 PUBLICATIONS **99** CITATIONS

SEE PROFILE

Dimitrios Papanastasiou
Foundation for Research and Technology -…
22 PUBLICATIONS **136** CITATIONS

SEE PROFILE

Vassileios Papadimitriou
University of Crete
30 PUBLICATIONS **378** CITATIONS

SEE PROFILE

Panos Papagiannakopoulos
University of Crete
66 PUBLICATIONS **656** CITATIONS

SEE PROFILE

Temperature-Dependent Rate Coefficients and Mechanism for the Gas-Phase Reaction of Chlorine Atoms with Acetone

MANOLIS N. ROMANIAS, VASSILEIOS G. STEFANOPOULOS, DIMITRIOS K. PAPANASTASIOU, VASSILEIOS C. PAPADIMITRIOU, PANOS PAPAGIANNAKOPOULOS

Laboratory of Photochemistry and Kinetics, Department of Chemistry, University of Crete, 71003, Heraklion, Crete, Greece

ABSTRACT: The rate coefficient for the gas-phase reaction of chlorine atoms with acetone was determined as a function of temperature (273–363 K) and pressure (0.002–700 Torr) using complementary absolute and relative rate methods. Absolute rate measurements were performed at the low-pressure regime ($\sim$2 mTorr), employing the very low pressure reactor coupled with quadrupole mass spectrometry (VLPR/QMS) technique. The absolute rate coefficient was given by the Arrhenius expression $k(T) = (1.68 \pm 0.27) \times 10^{-11} \exp[-(608 \pm 16)/T]$ cm^3 molecule^{-1} s^{-1} and $k(298$ K$) = (2.17 \pm 0.19) \times 10^{-12}$ cm^3 molecule^{-1} s^{-1}. The quoted uncertainties are the 2σ (95% level of confidence), including estimated systematic uncertainties. The hydrogen abstraction pathway leading to HCl was the predominant pathway, whereas the reaction channel of acetyl chloride formation (CH$_3$C(O)Cl) was determined to be less than 0.1%. In addition, relative rate measurements were performed by employing a static thermostated photochemical reactor coupled with FTIR spectroscopy (TPCR/FTIR) technique. The reactions of Cl atoms with CHF$_2$CH$_2$OH (3) and ClCH$_2$CH$_2$Cl (4) were used as reference reactions with $k_3(T) = (2.61 \pm 0.49) \times 10^{-11} \exp[-(662 \pm 60)/T]$ and $k_4(T) = (4.93 \pm 0.96) \times 10^{-11} \exp[-(1087 \pm 68)/T]$ cm^3 molecule^{-1} s^{-1}, respectively. The relative rate coefficients were independent of pressure over the

---

range 30–700 Torr, and the temperature dependence was given by the expression $k(T) = (3.43 \pm 0.75) \times 10^{-11} \exp[-(830 \pm 68)/T]$ cm^3 molecule^{-1} s^{-1} and $k(298\ K) = (2.18 \pm 0.03) \times 10^{-12}$ cm^3 molecule^{-1} s^{-1}. The quoted errors limits (2σ) are at the 95% level of confidence and do not include systematic uncertainties. © 2010 Wiley Periodicals, Inc. Int J Chem Kinet 42: 724–734, 2010

INTRODUCTION

Acetone is among the most important volatile organic compounds that have been detected in the troposphere, with mixing ratios in the range 300 ppt–3 ppb [1–3]. Acetone is considered as the main source of HO$_x$ radicals and is a precursor of peroxy acetyl nitrate in the upper troposphere, which contributes to the formation of tropospheric ozone [4–6]. Therefore, the kinetics and the degradation mechanism of acetone in the lower atmosphere is very important to the understanding of the ozone cycle in the troposphere. The primary removal of acetone from the troposphere occurs via photolysis, with a global estimate of ca. 64% [2,7]. However, chemical degradation through its reaction with OH radicals and NO$_3$ radicals, as well as with Cl atoms over the marine boundary layer, can also be of significant importance [7,8]. Finally, wet and/or dry deposition can amount in a smaller extent as a sink of acetone [7].

Although OH kinetics has been extensively studied and is well established, there are systematic discrepancies between relative rate methods [9–16] and absolute techniques, as far as the Cl kinetics is concerned [16,17]. The updated recommended room temperature value in the IUPAC review panel is based on the work from Orlando et al. [15] (relative rate measurement), which, although it is consistent with most of the relative rate results, is significantly lower compared to rate coefficients obtained using absolute rate techniques. Recently and while this work was in progress, Zhao et al. [17] measured the temperature dependence of the rate coefficient for the gas-phase reaction of Cl atoms with CH$_3$C(O)CH$_3$, employing the laser flash photolysis–resonance fluorescence (LFP-RF) technique. To the best of our knowledge, Zhao et al. (absolute rate coefficient determination) and Orlando et al. (relative rate methods) are the only studies existing in the literature that report temperature-dependent rate coefficients for the title reaction. Finally, there are few quantitative studies regarding the mechanism of the title reaction to evaluate the impact of Cl chemistry on the troposphere [18,19].

The aim of this work was to measure the rate coefficient for the gas-phase reaction of Cl atoms with acetone as a function of temperature (273–363 K) over a wide pressure range (0.002–700 Torr) using complementary absolute and relative rate techniques.

Moreover, the reaction pathways at the low-pressure regime (~2 mTorr) were quantitatively determined by quadrupole mass spectrometry. Finally, Cl chemistry contribution in atmospheric degradation of acetone is evaluated and discussed.

EXPERIMENTAL

Two different experimental setups were used during the course of this work:

1. Absolute rate coefficients determined employing the continuous flow system of very low pressure reactor (VLPR) coupled with a quadrupole mass spectrometer. Experiments were performed at the low-pressure regime (~2 mTorr) over the temperature range 273–363 K. The experimental setup has been extensively described elsewhere [20,21], and only a short description is given herein. The basic components of the VLPR system are (a) the double-wall Pyrex Knudsen reactor, (b) the 10-L glass storage bulbs used to continuously supply the Knudsen reactor with a steady flow of reacting gases through titrated buffer volumes and capillaries, (c) the Evenson cavity placed before reactor inlet used to produce Cl atoms via microwave discharge of Cl$_2$/He mixture flows, and (d) the quadrupole mass spectrometer and a filtering skimmer-mechanical tuning fork chopper used to discriminate and detect reactants and stable products.

2. The static thermostated photochemical reactor equipped with FTIR spectroscopy system (TPCR/FT-IR) was employed to determine the relative rate coefficients. A schematic of experimental setup is presented in Fig. 1. The basic components of TPCR/FT-IR are (a) the 100-cm-long jacketed cylindrical Pyrex reactor equipped with quartz windows at both ends, where the competing reactions occur, (b) the pulsed Nd:YAG laser (third harmonic, $\lambda = 355$ nm) used to produce Cl atoms by photolysis of 5% and/or 30% Cl$_2$/He mixtures, (c) the FT-IR system (Jasco 6300) used to analyze the reaction mixture, and (d) the circulation Teflon diaphragm pump was used to connect and
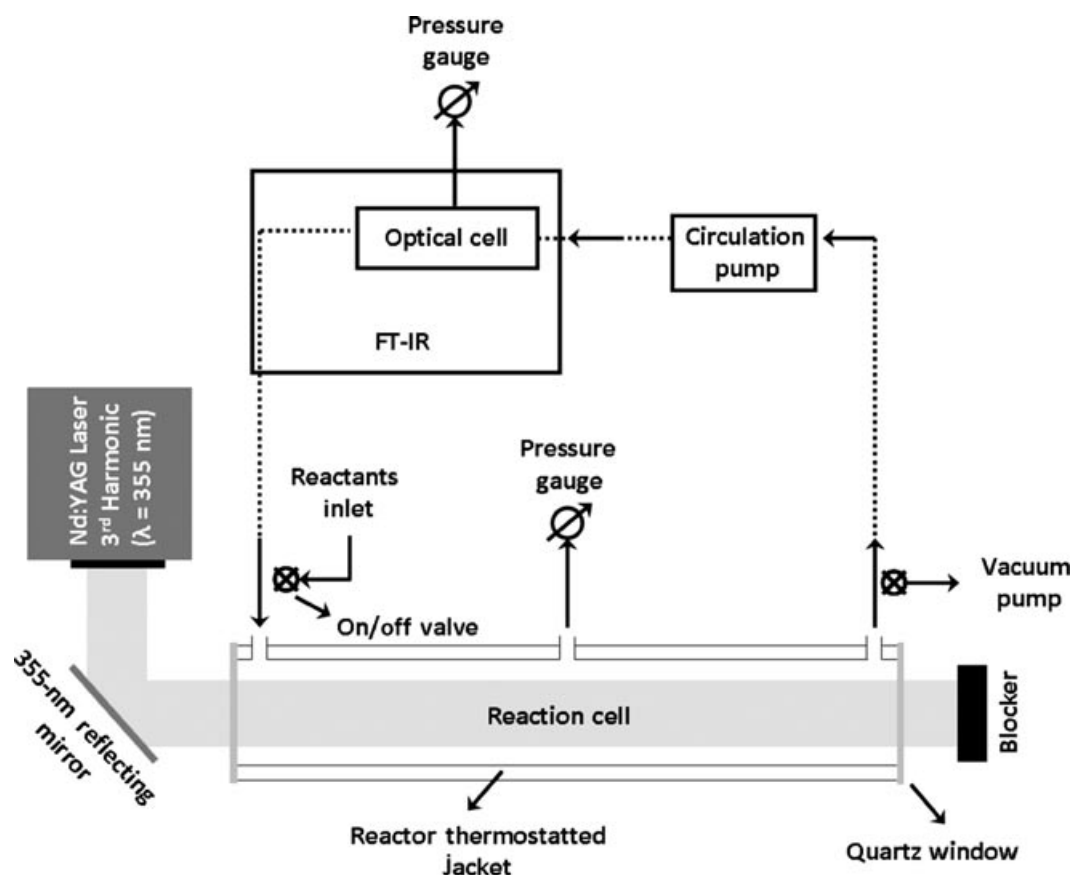
Figure 1   Simplified representation of the relative rate experimental setup used in the present work. Dashed line and solid arrows indicate the gas flow, and the component description is given as an inset.

ensure homogeneity between reaction and detection cell.

ABSOLUTE RATE COEFFICIENT MEASUREMENTS

The reaction occurred in a double-wall Knudsen reactor ($V = 109$ cm^3) that was internally coated with a thin layer of Teflon (FEP 121-A; DuPont, Geneva, Switzerland), to suppress wall reactions. The temperature was controlled by circulating water or methanol through the outer jacket (± 0.1 K). The steady-state concentration [M] of all reactants in the Knudsen reactor is proportional to the intensity I_M of their parent or prominent mass spectrometric peak and is given by the following expression:

$$[M] = F_M(k_{esc,M}V_{cell})^{-1} = I_M(\alpha_M \ V_{cell} \ k_{esc,M})^{-1} \quad (I)$$

where α_M is a mass spectrometric calibration factor and F_M is the flow rate of the reactant, which are determined with separate calibration experiments, as de-

scribed previously [20]. The escape rates $k_{esc,M}$ are given by the experimentally determined expression $2.66 \times (T/m)^{1/2}$ (s^{-1}) for a 5-mm escape orifice (T, temperature and m, molecular mass of reactant M), and the residence times of Cl and $CH_3C(O)CH_3$ species were 128 and 164 ms, respectively. The total pressure inside the reactor was less than 3 mTorr. The mass spectrum of acetone was taken at 19 eV and consists of three major peaks at $m/z = 58$, 43, and 15, among which the parent peak at m/z 58 was selected for monitoring acetone (free of any contribution from possible reaction products). The mass spectrum of acetyl chloride ($CH_3C(O)Cl$) was also taken at 19 eV and consists of three major fragment peaks at $m/z = 63$, 43, and 15, among which the peak at m/z 63 was selected for monitoring acetyl chloride. The detection limit for acetyl chloride ($S/N = 1$) in our system was determined to be ca. 5×10^8 molecules cm^{-3}.

Chlorine atoms were produced by a microwave discharge in a mixture of 5% Cl_2 in helium flowing through a quartz tube coated with a phosphoric–boric acid mixture, to inhibit chlorine atom recombination.

The decomposition of Cl_2 was complete, and this was verified by monitoring the mass peak at $m/e = 70$ at all times. The ionization electron energy was set at 19 eV to eliminate HCl fragmentation ($<0.3\%$) and its contribution to mass peak $m/e = 35$ (Cl^+), which always though was measured and taken into account.

The steady-state concentrations of reactants were in the range $[Cl] = (3–27) \times 10^{11}$ molecules cm^{-3} and $[CH_3C(O)CH_3] = (0.2–11) \times 10^{12}$ molecules cm^{-3}. The mass spectral intensities were measured with an uncertainty of ca. 5%.

RELATIVE RATE COEFFICIENT MEASUREMENTS

The competing reactions of Cl atoms with acetone (actn) and two reference compounds, CHF_2CH_2OH and $ClCH2CH2Cl$ (ref), took place in a thermostated cylindrical Pyrex reactor (100-cm long) equipped with quartz windows at both ends to be transparent to UV light. Chlorine atoms produced by pulsed laser photolysis of 5% (at high pressures) or 30% (at low-pressure conditions) of Cl_2/He mixtures using the third harmonic of a Nd:YAG laser ($\lambda = 355$ nm, ~ 60 mJ pulse^{-1}, 10 Hz). Reaction mixtures analyzed with Fourier transform infrared spectroscopy, using a separate 15-cm-long detection cell sealed with KBr windows. The pressure was continuously measured at the center of both cells using differential pressure transducers (DP15-30 and DP15-40), while temperature was regulated by circulating water or methanol through the double wall of the reactor. A Teflon diaphragm pump was used to interconnect reaction and detection cell in a closed loop and to ensure homogeneity in both volumes. The homogeneity was verified by recording sequential IR spectra until the intensity of the characteristic IR bands of the reactants was found to be steady. The typical time needed was ~ 20 min. All IR spectra used in kinetic determinations correspond to the average of 20 coadded samples recorded with resolution, $R = 1$ cm^{-1}.

Initially, experiments were performed to ensure that both acetone and reference compounds were not removed photolytically or via heterogeneous processes over the temperature range 273–363 K. Therefore, the IR spectrum of reaction mixtures was recorded at discrete time intervals for a time period of ca. 2 h and it was verified that no significant variation in their IR spectrum was observed. In addition, no detectable loss for acetone and reference reactants was observed by irradiating the reaction mixtures with 30,000 laser pulses ($\lambda = 355$ nm) for 1 h, in the absence of Cl atoms precursors (Cl_2/He mixture).

In a typical kinetic experiment, reactants, Cl precursors, and bath gas (N_2, synthetic air 80% N_2–20% O_2) used to balance the reaction mixture at the desirable pressure were introduced and mixed for at least 20 min. Most experiments were performed in excess of O_2 to scavenge the produced radicals and inhibit chain reactions that can result in secondary loss of reactants, by processes other than their reaction with Cl atoms. After recording the initial IR spectrum, the mixture was exposed to approximately 1000–2000 laser pulses ($\lambda = 355$ nm) and the relative losses of acetone and reference compound were recorded, once the homogeneity was confirmed. The procedure was repeated for reactant conversions in the range 10–80%. Single measurement experiments were also performed, in which the conversions occurred exposing a fresh sample each time with appropriate number of pulses, to keep the experimental time short and ascertain the absence of any significant side loss of the reactants.
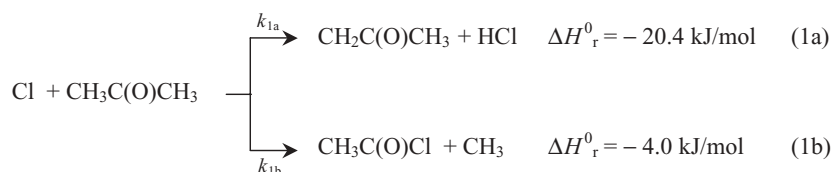
Materials

The chemicals used were commercially available, and their stated purity was 99.8% $CH_3C(O)CH_3$ (Merck, Darmstadt, Germany), >98% $CH_3C(O)Cl$ (Merck), 99.9993% He (Linde, Munich, Germany), 99.7% Cl_2 (Linde), 95% CHF_2CH_2OH (Fluorochem, Derbyshire, UK), and 99.8% $ClCH_2CH_2Cl$ (Merck). All reactants were degassed through several freeze–pump–thaw cycles at 77 K prior to use.

RESULTS

Absolute Rate Coefficients

The reaction of Cl atoms with acetone may proceed via the following reaction pathways:

$$Cl + CH_3C(O)CH_3 \begin{cases} \xrightarrow{k_{1a}} CH_2C(O)CH_3 + HCl & \Delta H^0_r = -20.4 \text{ kJ/mol} \quad (1a) \\ \xrightarrow{k_{1b}} CH_3C(O)Cl + CH_3 & \Delta H^0_r = -4.0 \text{ kJ/mol} \quad (1b) \end{cases}$$

whereas the most probable secondary reaction is

$$Cl + CH_3C(O)Cl \rightarrow CH_2C(O)Cl + HCl \quad (2)$$

with a rate coefficient $k_2 < 1 \times 10^{-14}$ cm^3 molecule^{-1} s^{-1} [22]. The reaction enthalpies ΔH_r° at 298.15 K were estimated by adopting literature values for the heats of formation ΔH_f° for all the reactants [21]. The secondary reaction of Cl atoms with acetonyl radical is not probable, due to the low-pressure conditions inside the reactor.

The mass spectrometric analysis of the reaction products showed the appearance of only one new mass peak at $m/e = 36$ (HCl$^+$), and there was no mass peak at $m/e = 63$, indicating the absence of CH$_3$C(O)Cl. It was also observed that an increase in the steady-state concentration of acetone resulted in Cl atom consumption and HCl production.

The steady-state condition for chlorine atoms yields the following expression:

$$\Delta[Cl]k_{esc,Cl} = k_1[Cl][Acetone] \quad (II)$$

where $\Delta[Cl] = [Cl]_o - [Cl]_r$ and $k_{esc,Cl}$ is the escape rate of chlorine atoms (subscripts o and r denote the absence or presence of acetone molecules, respectively). Rearrangement of the above expression gives

$$(R - 1)k_{esc,Cl} = k_1[Acetone]$$

where $R = [Cl]_o/[Cl]_r = I_{35,o}/I_{35,r}$. A typical plot of the above-mentioned equation at $T = 298$ K is presented in Fig. 2. The linear least-squares fit to the data
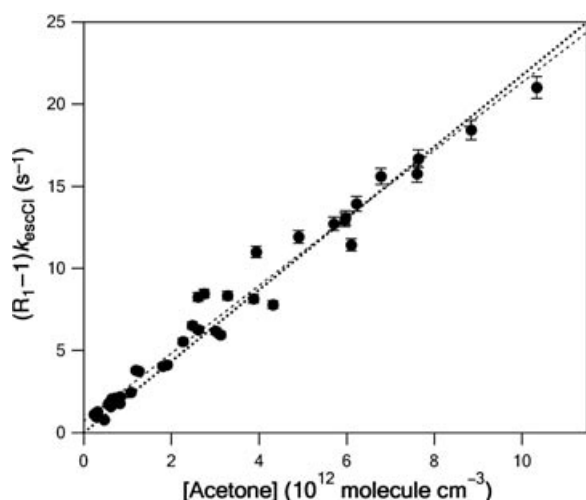
Figure 2 Typical plot of $(R_1-1)k_{esc,Cl}$ versus [Acetone] at $T = 298$ K. Error bars reflect the precision of each measurement at 95% level of confidence. The dotted line represents the forced to zero least-squares fit, and the dashed line represents the unrestricted least-squares fit.

yields the rate coefficient k_1. The 2σ precision of the fit of $(R - 1)k_{esc,Cl}$ versus [Acetone] was always better than 2%. The least-squares fit of the data was also taken without zero-forcing restrictions (see Fig. 2), and the obtained rate coefficient values were in excellent agreement (~2%) with the previous values. The intercepts were always lower than 3%.

Experiments were performed at four different temperatures 273, 298, 333, and 363 K, and the obtained absolute rate coefficients are given in Table I. The quoted error limits represent the 2σ and include systematic uncertainties. The error analysis and the estimated systematic uncertainties of the VLPR system (ca. 9%) have been described extensively elsewhere [20], and no peculiarities were observed in the measurements presented herein. A summary of the results at all temperatures is given in Table I.

Table I Absolute Rate Coefficients at Various Temperatures, Employing Different Experimental Conditions (Acetone and Cl Atom Concentration, Ratio $R_{Cl} = I_{Cl,0}/I_{Cl,r}$)

T (K)	[Acetone]^a	[Cl]^a	R_{Cl}	k_1 ($\times 10^{-12}$ cm^3 molecule^{-1} s^{-1})
273	0.19–9.21	5.29–7.43	1.04–3.40	1.95 ± 0.04
273	3.62–9.15	5.82–10.1	1.78–3.23	1.73 ± 0.10
273	0.59–7.83	5.34–7.1	1.14–2.83	1.93 ± 0.13
273	0.22–11.33	4.83–16.1	1.08–3.57	1.72 ± 0.05
273	0.77–7.24	6.23–16.0	1.20–2.82	1.91 ± 0.11
273	0.91–7.67	4.25–12.71	1.25–3.00	1.92 ± 0.11
		k_1(273 K) = 1.82 ± 0.15		
298	0.26–7.37	3.65–12.21	1.12–3.28	2.48 ± 0.18
298	0.84–13.72	3.5–13.84	1.25–4.74	2.12 ± 0.11
298	0.47–7.34	4.2–12.72	1.08–2.78	2.10 ± 0.22
298	0.23–9.14	7.35–27.45	1.12–3.76	2.44 ± 0.14
298	0.62–7.67	7.31–9.26	1.18–2.14	2.18 ± 0.17
		k_1(298 K) = 2.17 ± 0.19		
333	0.26–8.36	5.73–20.21	1.11–3.86	2.90 ± 0.12
333	1.53–9.75	3.73–7.25	1.58–4.05	2.66 ± 0.15
333	0.45–7.58	2.98–8.82	1.17–3.37	2.60 ± 0.08
333	0.50–6.12	2.98–3.15	1.23–1.91	2.59 ± 0.18
		k_1(333 K) = 2.70 ± 0.28		
363	1.49–5.33	5.71–10.71	1.61–2.86	3.11 ± 0.13
363	0.42–7.15	2.98–9.09	1.51–3.53	3.34 ± 0.36
363	0.43–1.94	8.56–12.82	1.17–1.86	3.83 ± 0.13
363	0.51–7.63	2.98–9.09	1.22–4.07	3.12 ± 0.18
		k_1(363 K) = 3.17 ± 0.28		

The quoted uncertainties are at 95% level of confidence and refer only to the precision of the R_{Cl} versus [CH$_3$C(O)CH$_3$] fit. The k_1 values at the bottom of each temperature represent the slope of the fit to all experimental data at that temperature; the quoted uncertainties include estimated systematic errors.

^{a}Cl atoms and CH$_3$C(O)CH$_3$ concentrations referred in 10^{11} and 10^{12} molecules cm^{-3}, respectively.

Experimental data were also analyzed based on acetone and HCl steady-state using the following expressions:

$$\Delta[\text{Acetone}]\, k_{\text{esc,Acetone}} = k_1[\text{Cl}][\text{Acetone}] \quad \text{(III)}$$

$$\Delta[\text{HCl}]\, k_{\text{esc,HCl}}/[\text{Cl}] = k_{1a}[\text{Acetone}] \quad \text{(IV)}$$

where $\Delta[\text{Acetone}] = [\text{Acetone}]_o - [\text{Acetone}]_r$ is the difference in acetone concentration in the absence and presence of Cl atoms, $\Delta[\text{HCl}] = [\text{HCl}]_r - [\text{HCl}]_{bg}$ is the difference between the produced HCl concentration via reaction (1) and the background HCl concentration, $k_{\text{esc,Acetone}}$ and $k_{\text{esc,HCl}}$ are the escape rate coefficients for acetone and HCl molecules, respectively, and [Cl] and [Acetone] are the steady-state concentrations for Cl atoms and acetone, respectively. To determine [Cl], the flow rate of chlorine atoms (F_{Cl}) was derived by assuming a mass balance for all chlorinated species in the discharge tube and the reactor, in the absence of any reactants. The mass balance is given by the following expression: $2 \times \Delta F_{\text{Cl2}} = F_{\text{Cl}} + F_{\text{HCl}}$, where ΔF_{Cl2} is the change in the flow rate of Cl_2 when the microwave discharge was turned on, whereas F_{Cl} and F_{HCl} are the flow rates of Cl and HCl, respectively. The mass spectrometric sensitivity of Cl atoms was determined relative to that for HCl, whose a_{HCl} factor was determined by calibration plots of a mixture of 5% HCl in He. The ratio ($a_{\text{HCl}}/a_{\text{Cl}}$) was determined by titration experiments using the simple reaction of Cl atoms with hexane, $n\text{-C}_6\text{H}_{14}$, and it was found to be 1.3 ± 0.1. Thus, the flow rate F_{Cl} was obtained by using the expression: $F_{\text{Cl}} = (2 \times \Delta F_{\text{Cl}_2}/[1 + I_{\text{HCl}}/(a_{\text{HCl}}/a_{\text{Cl}} \times I_{\text{Cl}})]$. Results obtained from data analysis based on Eqs. (III) and (IV) were in very good agreement with the ones determined based on Cl atoms steady state and were always agreed within 5%. The mass balance among reactants as well as among reactants and major reaction product HCl was excellent, which indicates that there is no significant secondary loss of Cl atoms and that the HCl production pathway is the major channel for the title reaction. Mass balance and kinetic measurements suggest that the contribution of channel 1b is less than 10%, which is the uncertainty of our measurements. Typical plots based on HCl and $\text{CH}_3\text{C(O)CH}_3$ steady states are given in the Supporting Information (Figs. S1 and S2).

The temperature dependence of the rate coefficient is very well represented by the expression $k(T) = (1.68 \pm 0.27) \times 10^{-11}\, \exp[-(608 \pm 16)/T]\, \text{cm}^3$ $\text{molecule}^{-1}\, \text{s}^{-1}$. The Arrhenius plot is given in Fig. 4. Arrhenius parameters and corresponding errors were estimated from the linear least-square analysis of $\ln k$ as a function of the reversed temperature ($1000/T$). The uncertainties in the exponential part of the Arrhenius expressions reflect the 2σ precision of the least-squares fits, whereas the uncertainties in preexponential factors were estimated by the expression $\text{d}\,A = A \times \text{d}\ln A$, taking also into account the systematic errors of the measurements. The uncertainties were also expressed in terms of the NASA/JPL recommendation [23], for reference purposes, and are presented in Fig. S3 in the Supporting Information.

To improve the accuracy of the upper limit that reaction pathway 1b contributes in the reaction scheme, the steady-state kinetic expression for acetyl chloride was also employed in combination with the detection limit of acetyl chloride determined in the present work (5×10^8 molecules cm^{-3}):

$$\Delta[\text{AcetylCl}]\, k_{\text{esc,AcetylCl}} = k_{1b}[\text{Cl}][\text{Acetone}]$$
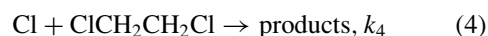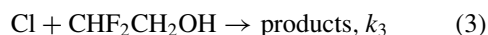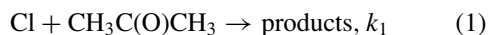$$+ k_2[\text{Cl}][\text{AcetylCl}] \quad \text{(V)}$$

where [AcetylCl] and [Acetone] are the steady-state concentrations of acetyl chloride and acetone, respectively. The $k_{\text{esc,AcetylCl}}$ value at room temperature is $5.20\, \text{s}^{-1}$. Rearrangement of the above expression leads to

$$[\text{AcetylCl}] = k_{1b}[\text{Cl}][\text{Acetone}]/\{k_{\text{esc,ActCl}} + k_2[\text{Cl}]\}$$
$$= k_{1b}[\text{Cl}][\text{Acetone}]/k_{\text{esc,ActCl}}$$

since $k_2[\text{Cl}] \ll k_{\text{esc,AcetylCl}}$. Knowing that the detection limit of acetyl chloride in our experimental setup was $\sim 5 \times 10^8$ molecules cm^{-3}, the above expression provides an upper limit for k_{1b}, which is $1.4 \times 10^{-15}\, \text{cm}^3$ $\text{molecule}^{-1}\, \text{s}^{-1}$. The Cl atoms and acetone concentrations are given in Table I. The above upper limit value of k_{1b} indicates that the reaction yield for channel 1b is less than 0.1% over the examined pressure and temperature regime.

Relative Rate Coefficients

The basic concept in relative rate determination is to follow the relative loss rates of the primary reactant (acetone) and the reference compound (ref), considering that it is solely due to their gas-phase reaction with Cl atoms. In our experiments, $\text{CHF}_2\text{CH}_2\text{OH}$ and $\text{ClCH}_2\text{CH}_2\text{Cl}$ were the reference compounds; therefore, the reaction scheme is

$$\text{Cl} + \text{CH}_3\text{C(O)CH}_3 \rightarrow \text{products}, k_1 \quad \text{(1)}$$

$$\text{Cl} + \text{CHF}_2\text{CH}_2\text{OH} \rightarrow \text{products}, k_3 \quad \text{(3)}$$

$$\text{Cl} + \text{ClCH}_2\text{CH}_2\text{Cl} \rightarrow \text{products}, k_4 \quad \text{(4)}$$

from which the rate coefficients are related via the following expression:

$$\ln\left(\frac{[\text{Acetone}]_0}{[\text{Acetone}]_t}\right) = \frac{k_1}{k_{\text{ref}}} \ln\left(\frac{[\text{ref}]_0}{[\text{ref}]_t}\right) \qquad \text{(VI)}$$

where the indices 0 and t refer to the initial and at time t concentrations of acetone and reference compounds, respectively.

The rate coefficient k_3 as a function of temperature was determined by Papadimitriou et al. [24] and is given by the expression $k_3(T) = (2.61 \pm 0.49) \times 10^{-11}$ $\exp[-(662 \pm 60)/T]$ cm^3 molecule^{-1} s^{-1}. The temperature dependence of k_4 was determined by Tschuikow-Roux et al. [25] and is given by the expression $k_4(T) = (4.93 \pm 0.96) \times 10^{-11}$ $\exp[-(1087 \pm 68)/T]$ cm^3 molecule^{-1} s^{-1}. The relative rate measurements are summarized in Table II. The rate coefficients were obtained by taking the average value of the values derived from two reference compounds. The quoted uncertainties include the extremes of estimated uncertainties of reference reactions. Rate coefficients were independent of pressure in the range 30–700 Torr. The room temperature value was found to be $k_1(298 \text{ K}) = (2.18 \pm 0.03) \times 10^{-12}$ cm^3 molecule^{-1} s^{-1}, where the quoted error limits are at the 95% level of confidence and refer to the precision of the fit. A typical plot for all measurements employing relative rate method at $T = 298$ K, using the two different compounds, is presented in Fig. 3. The excellent agreement between the room temperature k values obtained via both experimental techniques clearly shows that there is no measurable pressure dependence of the rate coefficient in the range 2 mTorr–700 Torr and therefore there is no intermediate adduct formation channel in the mechanistic reaction scheme. It also provides additional evidence about the validity of our rate coefficient measurements, since two independent experimental setups result in almost identical k values, therefore excluding any probable intrinsic artifacts in the two experimental techniques. The rate coefficient values of k_1 at four temperatures are given in Table II. The temperature dependence of reaction rate coefficient determined employing relative rate methods is represented very well by the expression $k(T) = (3.43 \pm 0.75) \times 10^{-11}$ $\exp[-(830 \pm 68)/T]$ cm^3 molecule^{-1} s^{-1}, which is slightly but not negligibly different than the one determined using the VLPR measurements. The quoted uncertainties are the 2σ precision of the fits. Although the precision of our relative rate measurements is high, it is worth noticing that the rate coefficients obtained using the relative rate method depends strongly on the selected reference compound. The high uncertainties in the rate coefficients of the reference compounds reported at temper-
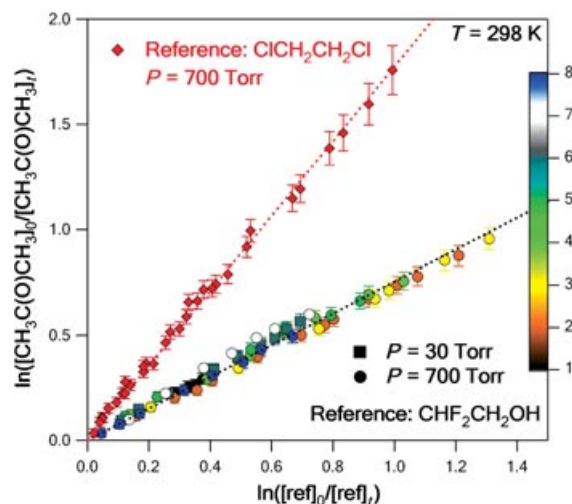
Figure 3 Relative rate coefficients ratios obtained at room temperature, $T = 298$ K, for the title reaction, using CHF$_2$CH$_2$OH ($P = 30$ Torr, solid squares and $P = 700$ Torr, solid circles) and ClCH$_2$CH$_2$Cl (red solid triangles) as reference compounds. The dashed lines are the linear least-squares fit of $\ln([\text{CH}_3\text{C(O)CH}_3]_0/[\text{CH}_3\text{C(O)CH}_3]_t)$ versus $\ln([\text{ref}]_0/[\text{ref}]_t)$ that yield $r_1 = 0.75 \pm 0.01$ and 1.78 ± 0.02, respectively. The quoted error limits are the 2σ uncertainty in the precision of the slope. The color coding in CH$_3$C(O)CH$_3$ versus CHF$_2$CH$_2$OH data sets designates different series of experiments. Data quality is representative for repeatability and precision of the measurements. [Color figure can be viewed in the online issue, which is available at wileyonlinelibrary.com]

atures away from room temperature, mainly because of experimental difficulties [23], unavoidably result in higher error limits and lower confidence. Note that the uncertainty in k_{ref} is inherent in all the reaction rate coefficients determined, employing relative rate methods on the top of our estimated systematic errors. Moreover, even though it is highly unlikely to observe any pressure dependence in the rate coefficients of the used reference compounds, it is necessary to measure their absolute rate coefficients over the examined pressure regime. Therefore, the temperature dependence of the reaction rate coefficient is more accurately represented by giving the expression obtained using the absolute rate coefficient measurements.

DISCUSSION AND CONCLUSIONS

The total absolute rate coefficient for the reaction of Cl atoms with acetone was measured at four different temperatures in the range 273–363 K, and the room temperature rate coefficient value is $k_1(298 \text{ K}) = (2.17 \pm 0.19) \times 10^{-12}$ cm^3 molecule^{-1} s^{-1}. In addition, relative rate coefficients determined in the same

Table II Relative Rate Coefficients and k_1/k_{ref} at Various Temperatures, Employing Different Experimental Conditions (Total Pressure, Cl_2, Acetone, CHF_2CH_2OH, and $ClCH_2CH_2Cl$ Concentrations)

Temperature (K)	Pressure (Torr)[a]	$[Cl_2]^b$	$[CH_3COCH_3]^b$	$[Reference]^b$	$r:(k_1/k_{ref})$	$k_1 \pm 2\sigma^c$
		Reference reaction: $Cl + CHF_2CH_2OH$ (k_3)				
273	25	11.0	6.50	6.4	0.73 ± 0.01	1.54 ± 0.02
273	700	19.0	6.40	4.90	0.70 ± 0.01	1.61 ± 0.02
273	690	14.0	7.80	7.08	0.67 ± 0.01	1.54 ± 0.02
		Reference reaction: $Cl + ClCH_2CH_2Cl$ (k_4)				
273	700	10.0	3.24	2.59	1.84 ± 0.04	1.67 ± 0.04
273	700	9.0	3.24	2.27	1.94 ± 0.04	1.76 ± 0.03
		k_1(273 K) = (1.62 ± 0.49)				
		Reference reaction: $Cl + CHF_2CH_2OH$ (k_3)				
298	30	7.7	6.40	6.50	0.81 ± 0.01	2.29 ± 0.03
298	700	7.8	6.50	5.10	0.77 ± 0.01	2.18 ± 0.03
298	700	15.0	6.40	4.90	0.72 ± 0.01	2.04 ± 0.03
298	700	12.0	6.40	4.90	0.73 ± 0.01	2.06 ± 0.03
298	700	9.7	6.50	4.80	0.78 ± 0.03	2.21 ± 0.09
298	706	11.0	7.13	6.50	0.76 ± 0.02	2.15 ± 0.06
		Reference reaction: $Cl + ClCH_2CH_2Cl$ (k_4)				
298	700	12.0	6.48	5.00	1.74 ± 0.02	2.21 ± 0.03
298	700	10.0	3.24	2.27	1.78 ± 0.04	2.26 ± 0.05
298	700	11.5	5.00	3.24	1.75 ± 0.02	2.22 ± 0.02
		k_1(298 K) = (2.18 ± 0.65)				
		Reference reaction: $Cl + CHF_2CH_2OH$ (k_3)				
333	700	17.0	6.40	4.90	0.77 ± 0.01	2.78 ± 0.04
333	723	10.0	7.25	7.54	0.76 ± 0.01	2.76 ± 0.04
333	730	10.0	6.50	4.80	0.75 ± 0.01	2.73 ± 0.04
		Reference reaction: $Cl + ClCH_2CH_2Cl$ (k_4)				
333	700	12.0	3.00	2.59	1.56 ± 0.04	2.92 ± 0.07
333	700	11.5	4.50	3.24	1.53 ± 0.02	2.86 ± 0.04
		k_1(333 K) = (2.81 ± 0.86)				
		Reference reaction: $Cl + CHF_2CH_2OH$ (k_3)				
363	30	7.8	6.60	6.80	0.87 ± 0.01	3.66 ± 0.04
363	700	13.0	6.40	4.90	0.77 ± 0.01	3.26 ± 0.04
363	700	9.6	6.65	6.90	0.87 ± 0.03	3.66 ± 0.04
		Reference reaction: $Cl + ClCH_2CH_2Cl$ (k_4)				
363	700	10.0	3.24	2.27	1.40 ± 0.04	3.42 ± 0.10
363	700	12.5	3.55	2.7	1.41 ± 0.02	3.44 ± 0.06
		k_1(363 K) = (3.49 ± 1.04)				

The quoted uncertainties in k_1/k_{ref} are at 95% level of confidence and refer to the precision of the $\ln([CH_3C(O)CH_3]_0/[CH_3C(O)CH_3]_t)$ versus $\ln([ref]_0/[ref]_t)$ fit. The k_1 values at the bottom of each temperature represent the average of all experimental values obtained using both reference compounds; the quoted uncertainties include the extremes of the quoted error limits in reference rate coefficients.

[a] All experiments performed with synthetic air (80% N_2 / 20% O_2) as a bath gas unless otherwise noted. k_3($Cl + CHF_2CH_2OH$) in 10^{-12} cm^3 $molecule^{-1}$ s^{-1}: k_3(273 K) = (2.31 ± 0.38), k_3(298 K) = (2.83 ± 0.39), k_3(333 K) = (3.61 ± 0.41), and k_3(363 K) = (4.24 ± 0.69). k_4($Cl + ClCH_2CH_2Cl$) in 10^{-12} cm^3 $molecule^{-1}$ s^{-1}: k_4(273 K) = (9.10 ± 2.70), k_4(298 K) = (1.28 ± 0.38), k_4(333 K) = (1.87 ± 0.56), and k_4(363 K) = (2.44 ± 0.72) (quoted errors are the ~30% uncertainty of the rate coefficient value as authors estimated at room temperature).

[b] Concentrations referred in 10^{16} molecules cm^{-3}.

[c] k referred in 10^{-12} cm^3 $molecule^{-1}$ s^{-1} and the quoted uncertainty is the 2σ precision of the fit.

temperature range but extended the pressure range up to 700 Torr. The room temperature rate coefficient determined to be k_1(298 K) = (2.18 ± 0.03) × 10^{-12} cm^3 $molecule^{-1}$ s^{-1}, where the quoted error is the 2σ precision of the fit and does not include systematic uncertainties. The results from this study can be compared with the respective ones reported by other groups, which are presented in Table III. Our room temperature k_1 values derived using both experimental techniques are in excellent agreement, and they are

Table III   Room Temperature Rate Coefficient and Arrhenius Parameters for the Reaction of Cl Atoms with Acetone Using Absolute and Relative Techniques

$k_1 \pm 2\sigma$ (298 K)[a]	A[b]	E_a/R[c]	Pressure Range[d]	Technique	Reference
			Absolute rate coefficients		
3.06 ± 0.38			15–60	PLP-RF	Notario et al. [13]
2.93 ± 0.20			20–200	PLP-RF	Albaladejo et al. [9]
2.00 ± 0.30	1.53 ± 0.19	594 ± 33	30–300	LFP-RF	Zhao et al. [17]
2.17 ± 0.19	1.68 ± 0.27	608 ± 16	$\sim 2 \times 10^{-3}$	VLPR	This work
			Relative rate coefficients		
2.02 ± 0.30	1.52 ± 0.16	628 ± 150	760	RR	Orlando et al. [15]
1.69 ± 0.32			760	RR	Olsson et al. [14]
2.07 ± 0.12			700	RR	Christensen et al. [12][e]
2.25 ± 0.08			700	RR	Christensen et al. [12][e]
2.15 ± 0.04			700	RR	Christensen et al. [12][e]
2.22 ± 0.05			700	RR	Christensen et al. [12][e]
2.00 ± 0.09			700	RR	Sellevåg et al. [26]
2.12 ± 0.05			700–760	RR	Carr et al. [11]
2.18 ± 0.03	3.43 ± 0.75	830 ± 35	30–700	RR	This work

Abbreviations: PLP-RF, pulsed laser photolysis–resonance fluorescence; VLPR, very low pressure reactor; RR, relative rate.
[a]Rate coefficients are given in 10^{-12} cm^3 molecule^{-1} s^{-1}.
[b]Preexponential factors are given in 10^{-11} cm^3 molecule^{-1} s^{-1}.
[c]E_a/R is given in K.
[d]Pressure is given in Torr.
[e]Different reference reactions used at each measurement of Christensen et al.

also in excellent agreement with the values reported previously in the literature using the relative rate methods and the recent value of Zhao et. al. obtained using an absolute rate method [17]. All rate coefficient values and Arrhenius parameters known in the literature are given in Table III, and they are presented in an Arrhenius plot for direct comparison purposes in Fig. 4. Our study resolves the systematic discrepancy between the absolute rate measurements [9,13,17] and the consistently lower (ca. 1.3 times) relative rate determinations [11,12,14,15,26]. This systematic discrepancy cannot be easily resolved, since a great variety of reference compounds have been used in the relative rate measurements, which produce results with limited scattering. Moreover, the absolute rate coefficient measurements were performed with great care and it is difficult to evaluate possible intrinsic errors. In addition, the VLPR experiments show an excellent mass balance between Cl atoms and HCl product, as well as between Cl atoms and acetone, which provides strong evidence about the validity of our absolute rate measurements. In particular, the values obtained by monitoring the appearance of HCl concentration were equal within experimental error, with the values obtained by monitoring the concentrations of both reactants. Furthermore, the excellent mass balance between Cl atoms and HCl is an additional indication that the major reaction pathway via the title reaction occurs is the direct hydrogen atom abstraction. Yield measurements for re-

action pathway 1b revealed that the upper limit for the adduct-formation pathway (reaction (1b)) is less than 0.1%, in the temperature range 273–363 K and at the very-low-pressure regime (<3 mTorr).
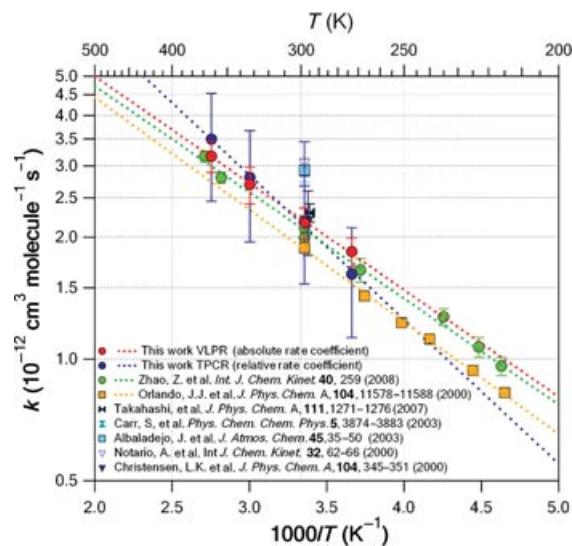
Figure 4   The Arrhenius plot of the title reaction; it includes all available in literature values and present values. Red and blue solid circles values obtained by this work, employing absolute (VLPR) and relative (TPCR/FTIR) rate methods, respectively. The source of all values is given as inset in the diagram. Red and blue dotted lines are the least-squares fits of our experimental values. [Color figure can be viewed in the online issue, which is available at wileyonlinelibrary.com.]

The E_a/R value (608 ± 16) K, obtained by absolute rate measurements, is in excellent agreement with the value (594 ± 33) K reported by Zhao et al. [17]. Moreover, there is satisfactory agreement with the value (628 ± 25) K obtained by Orlando et al. [15], by accepting the latest NASA/JPL Arrhenius expression for the reference reaction of Cl atoms with CH_2Cl_2. The new Arrhenius expression of Orlando et al. [15] becomes $k_1(T) = (1.52 \pm 0.16) \exp(-628 \pm 25/T)$ cm^3 $molecule^{-1}$ s^{-1}. The discrepancy between our E_a/R values, obtained by using the absolute and the relative rate methods, is probably due to the presence of additional uncertainties in relative rate measurements (uncertainties in measuring k_2 and k_3). Furthermore, our pre-exponential A factor value $(1.53 \pm 0.19) \times 10^{-11}$ cm^3 $molecule^{-1}$ s^{-1}, obtained by absolute rate measurements, is in excellent agreement with the values $(1.68 \pm 0.27) \times 10^{-11}$ cm^3 $molecule^{-1}$ s^{-1} and $(1.52 \pm 0.16) \times 10^{-11}$ cm^3 $molecule^{-1}$ s^{-1}, obtained by the absolute measurements of Zhao et al. [17] and the relative measurements of Orlando et al. [15], respectively. It is also noticed that our A factor values, using absolute and relative methods, differ by a factor of ~ 1.4, whereas the E_a/R values differ only by ca. 30%. This difference is probably due to the propagation of uncertainties, which are attributed to the reference reactions, especially at temperatures away from the room temperature.

Moreover, as far as the atmospheric implications of Cl chemistry in degradation of acetone in the troposphere is concerned, although their reaction is almost 10 times faster than the one initiated by OH radicals, Cl atoms are expected to be a minor but not negligible sink for acetone. Since the tropospheric concentration of Cl atoms over coastal areas is up to 3.4×10^4 molecules cm^{-3} [27], the atmospheric lifetime acetone due to its reaction with Cl atoms is 187 days. Considering that atmospheric lifetime of acetone is 1700 h due to photolysis, and 910 h due to reaction with OH radicals ($[OH] = 1.8 \times 10^6$ molecules cm^{-3} [28]), the contribution of the Cl chemistry to the removal of acetone from the troposphere is up to 11%. Therefore, the Cl atom chemistry should be probably taken into account in global atmospheric models to improve results and prediction accuracy. Finally, regarding the end products for the reaction of Cl atoms with acetone, the present work showed that there are no major chlorinated products other than HCl and thus tropospheric chlorine cannot be transported to the stratosphere in a form that can be adverse to the protective ozone layer.

BIBLIOGRAPHY

1. Jacob, D. J.; Field, B. D.; Jin, E. M.; Bey, I.; Li, Q.; Logan, J. A.; Yantosca, R. M.; Singh, H. B. J Geophys Res 2002, 107, 4100–4116.
2. Singh, H. B.; Kanakidou, M.; Crutzen, P. J.; Jacob, D. J. Nature 1995, 378, 50–54.
3. Singh, H. B.; O'Hara, D.; Herlth, D.; Sachse, W.; Blake, D. R.; Bradshaw, J. D.; Kanakidou, M.; Crutzen, P. J. J Geophys Res 1994, 99, 1805–1819.
4. Jaegle, L.; Jacob, D. J.; Brune, W. H.; Wennberg, P. O. Atmos Environ 2001, 35, 469–489.
5. McKeen, S. A.; Gierczak, T.; Burkholder, J. B.; Wennberg, P. O.; Hanisco, T. F.; Keim, E. R.; Gao, R.-S.; Liu, S. C.; Ravishankara, A. R.; Fahey, D. W. Geophys Res Lett 1997, 24, 3177–3180.
6. Wennberg, P. O.; Hanisco, T. F.; Jaegle, L.; Jacob, D. J.; Hintsa, E. J.; Lanzendorf, E. J.; Anderson, J. G.; Gao, R.-S.; Keim, E. R.; Donnelly, S. G.; Del Negro, L. A.; Fahey, D. W.; McKeen, S. A.; Salawitch, R. J.; Webster, C. R.; May, R. D.; Herman, R. L.; Proffitt, M. H.; Margitan, J. J.; Atlas, E. L.; Schauffler, S. M.; Flocke, F.; McElroy, C. T.; Bui, T. P. Science 1998, 279, 49–53.
7. Platt, U.; Allan, W.; Lowe, D. Atmos Chem Phys 2004, 4, 2393–2399.
8. Pszenny, A. A. P.; Fischer, E. V.; Russo, R. S.; Sive, B. C.; Varner, R. K. J Geophys Res 2007, 112, D10S13.
9. Albaladejo, J.; Notario, A.; Cuevas, C. A.; Ballesteros, B.; Martínez, E. J Atmos Chem 2003, 45, 35–50.
10. Atkinson, R.; Baulch, D. L.; Cox, R. A.; Crowley, J. N.; Hampson, R. F.; Hynes, R. G., Jr.; Jenkin, M. E.; Kerr, J. A.; Rossi, M. J.; Troe, J. IUPAC Subcommittee on Gas Kinetic Data Evaluation for Atmospheric Chemistry, Web Version February 2006. Retrieved December 7, 2006, from http://jpldataeval.jpl.nasa.gov.
11. Carr, S.; Shallcross, D. E.; Canosa-Mas, C. E.; Wenger, J. C.; Sidebottom, H. W.; Treacy, J. J.; Wayne, R. P. Phys Chem Chem Phys 2003, 5, 3874–3883.
12. Christensen, L. K.; Ball, J. C.; Wallington, T. J. J Phys Chem A 2000, 104, 345–351.
13. Notario, A.; Mellouki, A.; Le Bras, G. Int J Chem Kinet 2000, 32, 62–66.
14. Olsson, B. E. R.; Hallquist, M.; Ljungstrom, E.; Davidsson, J. Int J Chem Kinet 1997, 29, 195–201.
15. Orlando, J. J.; Tyndall, G. S.; Vereecken, L.; Peeters, J. J Phys Chem A 2000, 104, 11578–11588.
16. Sander, S. P.; Friedl, R. R.; Ravishankara, A. R.; Golden, D. M.; Kolb, C. E.; Kurylo, M. J.; Huie, R. E.; Orkin, V. L.; Molina, M. J.; Moortgat, G. K.; Finlayson-Pitts, B. J. JPL Publication 06-2; Jet Propulsion Laboratory, Pasadena, CA, 2006.
17. Zhao, Z.; Huskey, D. T.; Nicovich, J. M.; Wine, P. H. Int J Chem Kinet 2008, 40, 259–267.

18. Singh, H. B.; Kasting, J. F. J Atmos Chem 1998, 7, 261.

19. Finlayson-Pitts, B. J Res Chem Intermed 1993, 19, 235.

20. Papadimitriou, V. C.; Papanastasiou, D. K.; Stefanopoulos, V. G.; Zaras, A. M.; Lazarou, Y. G.; Papagiannakopoulos, P. J Phys Chem A 2007, 111, 11608–11617.

21. Papadimitriou, V. C.; Kambanis, K. G.; Lazarou, Y. G.; Papagiannakopoulos, P. J Phys Chem A 2004, 108, 2666–2674.

22. Shi, J.; Wallington, T. J.; Kaiser, E. W. J Phys Chem A 1993, 97, 6184–6192.

23. Sander, S. P.; Friedl, R. R.; Ravishankara, A. R.; Golden, D. M.; Kolb, C. E.; Kurylo, M. J.; Molina, M. J.; Moortgat, G. K.; Keller-Rudek, H.; Finlayson-Pitts, B. J.; Wine, P. H.; Huie, R. E.; Orkin, V. L. Evaluation Number 15, Publication 06-2; Jet Propulsion Laboratory (JPL), California Institute of Technology: Pasadena, CA, 2006.

24. Papadimitriou, V. C.; Prosmitis, A. V.; Lazarou, Y. G.; Papagiannakopoulos, P. J Phys Chem A 2003, 107, 3733–3740.

25. Tschuikow-Roux, E.; Faraji, F.; Niedzielski, J. Int J Chem Kinet 1986, 18, 513–527.

26. Sellevåg, S. R.; Nielsen, C. J Asian Chem. Lett 2003, 7, 15.

27. Wingenter, O. W.; Sive, B. C.; Blake, N. J.; Blake, D. R.; Rowland, F. S. J Geophys Res 2005, 110, D20308.

28. Davis, D.; Grodzinsky, G.; Chen, G.; Crawford, J.; Eisele, F.; Mauldin, L.; Tanner, D.; Cantrell, C.; Brune, W.; Tan, D.; Faloona, I.; Ridley, B.; Montzka, D.; Walega, J.; Grahek, F.; Sandholm, S.; Sachse, G.; Vay, S.; Anderson, B.; Avery, M.; Heikes, B.; Snow, J.; O'Sullivan, D.; Shetter, R.; Lefer, B.; Blake, D.; Blake, N.; Carroll, M.; Wang, Y. J Geophys Res 2001, 106, 32691–32707.